SOME CONSEQUENCES OF NON-LOCAL-EQUILIBRIUM IN HYPERSONIC AERODYNAMIC FLOWS

C.J. Greenshields, J.M. Reese
Department of Mechanical Engineering, University of Strathclyde, Glasgow, UK

In simulating high-speed, high-altitude aerodynamics it is important to be able to capture physical phenomena that are due to the non-local-equilibrium nature of the rarefied gas flow (this is in addition to any effects due to dissociation, ionisation and energy partition in diatomic molecules). The physical effects of the gas rarefaction can be particularly important close to any solid surface, where they have implications for the heat transfer and mechanical stresses experienced by the surface, and hence on the design of the leading edges and control surfaces of aerodynamic vehicles.

In this paper we focus on the non-equilibrium effect that is the velocity slip at surfaces. However, the Knudsen layer — characterised by strong departures from linearity of the stress/strain-rate relationship within one or two molecular mean free paths of a surface — should also be incorporated within any comprehensive numerical model, although it is still unclear how best to achieve this [1].

This paper represents the first outcomes of a new research programme in the UK on hypersonic computational aerodynamics. In particular, it describes an early observation of geometry dependence within the calculation of the velocity slip at surfaces that should be properly accounted for.

Geometry-dependence in the velocity slip boundary condition

The classical description of the velocity slip of rarefied gases flowing close to solid surfaces is due to Maxwell [2], and forms of this 'Maxwell slip condition' are widely implemented in current rarefied gas flow solvers, e.g. [3-5]. However, the generality of the condition originally proposed by Maxwell has been widely misinterpreted; Maxwell's expression is applicable for any geometry but the form in which it is generally presented and implemented in flow solvers is, strictly, only appropriate for a narrow set of specific geometries which may not be that of the aerodynamic flow situation under investigation.

Maxwell originally related the tangential gas velocity slip at a solid surface, $\vec{u}_{\text{slip}}$, to the tangential shear stress, $\vec{\tau}$, and heat flux, $\vec{q}$. Written in vector form so that it can be readily applied to flows over three-dimensional surfaces, the Maxwell slip condition is [2]

$$\vec{u}_{\text{slip}} = -\frac{(2-\sigma)}{\sigma\mu}\lambda\vec{\tau} - \frac{3}{4}\frac{N_{\text{Pr}}(\gamma-1)}{\gamma p}\vec{q}, \quad (1)$$

where $\vec{\tau} = (\vec{i}_n \cdot \mathbf{\Pi}) \cdot (\mathbf{1} - \vec{i}_n\vec{i}_n)$, $\vec{q} = \vec{Q} \cdot (\mathbf{1} - \vec{i}_n\vec{i}_n)$, an arrow denotes a vector quantity, σ is the tangential momentum accommodation coefficient, μ is the gas viscosity at the wall, λ is the molecular mean free path at the wall, N_{Pr} is the Prandtl number, γ is the specific heat ratio, p is the gas pressure at the wall, $\vec{i}_n$ is a unit vector normal and away from the wall $\mathbf{\Pi}$ is the stress tensor at the wall, $\mathbf{1}$ is the identity tensor, and $\vec{Q}$ is the heat flux vector at the wall.

Typically, the Navier-Stokes-Fourier (NSF) constitutive expressions are used for the viscous stress and heat flux terms in equation (1). Maxwell thereby obtained the following equation

$$u_{\text{s}} = \frac{(2-\sigma)}{\sigma}\lambda\frac{\partial u_x}{\partial n} - \frac{3}{4}\frac{\mu}{\rho T}\frac{\partial T}{\partial x}, \quad (2)$$

where n is the co-ordinate normal to the wall, x is the co-ordinate tangential to the wall, u_x is the x component of the gas velocity, u_s is the x component of the slip velocity, and ρ and T are the density and temperature of the gas at the wall, respectively. This is the form of the Maxwell slip condition implemented in the numerical solutions of, e.g., [3-5].

However, many surface geometries of most interest in aerodynamics have curvature (including some of the test cases studied in [3-5]). In these cases, the simple expression (2) is inapplicable because in its derivation Maxwell himself assumed a situation in which there is no streamwise variation in wall-normal velocity, i.e. this expression is only appropriate for flows next to non-rotating planar walls. (Although, in deriving (2), he did allow for variation of temperature along the surface.)

If equation (2) is used as a boundary condition in a computational aerodynamic simulation of the rarefied flow around a body that contains curved surface elements, or surface elements that are moving normally to the streamwise direction (e.g. ailerons or other control surfaces), the simulation may miss some important features of the flow, in particular, close to the surface. For example, for a surface in two dimensions (and again using the NSF constitutive relations), equation (1) becomes [6]

$$u_{\text{s}} = \frac{(2-\sigma)}{\sigma}\lambda\left(\frac{\partial u_x}{\partial n} + \frac{\partial u_n}{\partial x}\right) - \frac{3}{4}\frac{\mu}{\rho T}\frac{\partial T}{\partial x}, \quad (3)$$

where u_n is the gas velocity normal to the wall. The additional term featuring in equation (3) but not in equation (2) may have a significant influence on the velocity slip, and the overall accuracy of the numerical simulation of the flowfield.

The full Maxwell slip condition is equation (1). If we accept the physical basis on which it is derived [2] it is applicable to surfaces of any geometry. In this paper we therefore report our work on two different scenarios in which this geometry effect within the Maxwell slip has some marked consequences.

Low-speed cylindrical Couette flow

Recent analytical and molecular dynamics studies suggest that the velocity profile in a rarefied cylindrical Couette flow can become inverted [6]. In the case of a stationary outer cylinder and rotating inner cylinder, ‘inverted’ means that the radial velocity of the gas becomes greater farther away from the moving centre.

We have performed a simple isothermal calculation using a finite-difference discretization of the Navier-Stokes equations to examine the influence various boundary conditions have

on the velocity profile across the radius [6]. To ensure the flow is rarefied and the effects of non-equilibrium are important, a microflow case at STP was chosen. The inner and outer cylinders have radii of 3λ and 5λ, respectively, and the former has a tangential velocity approximately a third of the speed of sound. The gas is argon, and the accommodation coefficient, σ, is 0.1.

Figure 1 shows a comparison of the velocity profiles (non-dimensionalised by the tangential velocity of the inner cylinder) predicted using the standard no-slip conditions, the conventional slip condition (2), Maxwell's general slip condition (1), DSMC, and an analytical method referred to in [6].

DSMC predicts an inverted velocity profile, as does Maxwell's general slip condition (1). But the conventional slip condition (2) performs poorly and does not predict the velocity profile inversion in this curved geometry. This is entirely due to the geometrical dependence of slip being omitted in the conventional slip condition.

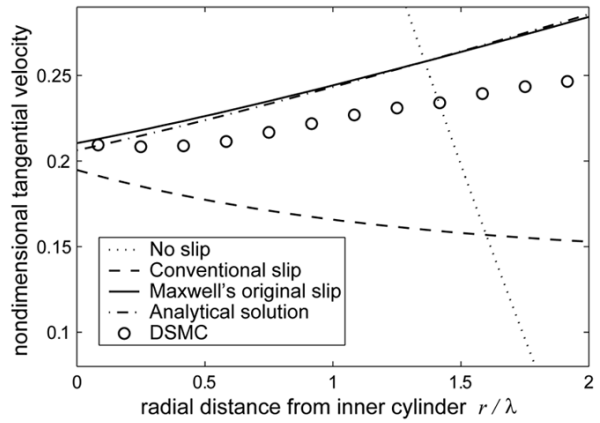

Fig. 1. Non-dimensional velocity profiles in cylindrical Couette flow [6]. Comparison of no-slip (···), conventional slip (- -), Maxwell's general slip (—), an analytical solution (· - ·) and DSMC data (o)

A cylinder in high-speed cross flow

Having shown that there are circumstances in which the geometry-dependence of the velocity slip is vital if we are to capture important flowfield phenomena properly, we now turn to investigate this effect at the macroscale — for high-speed rarefied flows.

The results reported here are the first outcomes of a new collaborative research programme between the University of Strathclyde and the Defence Science and Technology Laboratory in the UK on new approaches to computational hypersonic aerodynamics.

The benchmark case we investigate is the steady two-dimensional crossflow of air (gas constant 287 J/Kg K, ratio of specific heats 1.4, Prandtl number 0.71) at Mach 10 around a half cylindrical section of radius 0.05 m. The freestream temperature and pressure are 186 K and 0.7202 Pa, respectively, corresponding to a Knudsen number (ratio of molecular mean free path to the radius of curvature) of around 0.1. The gas is calorifically perfect, with a viscosity given by Sutherland's Law. The surface is assumed to be at a fixed temperature of 288 K, and accommodation coefficients of 0.85 are used for both velocity slip and temperature jump conditions at the surface.

This case may be considered analogous to the leading edge of aerodynamic control surfaces on high-speed/high-altitude vehicles. While it is a relatively simple 2D problem, the constant curvature over the leading edge is likely to lead to some differences between the final flowfield solution using Maxwell's general slip condition (1) compared with that using the conventional slip condition (2).

We are interested to know the extent to which the difference between the two forms of velocity slip boundary condition leads to an accumulation of error in velocity slip predictions along the surface — this error would then be passed on to affect predictions of performance of elements of the aerodynamic surface downstream.

For our simulations we fix the air stagnation temperature to be low (corresponding to that at around 80 km altitude) to isolate the effects of geometry-dependent slip from any effects due to molecular dissociation, ionisation and energy partition.

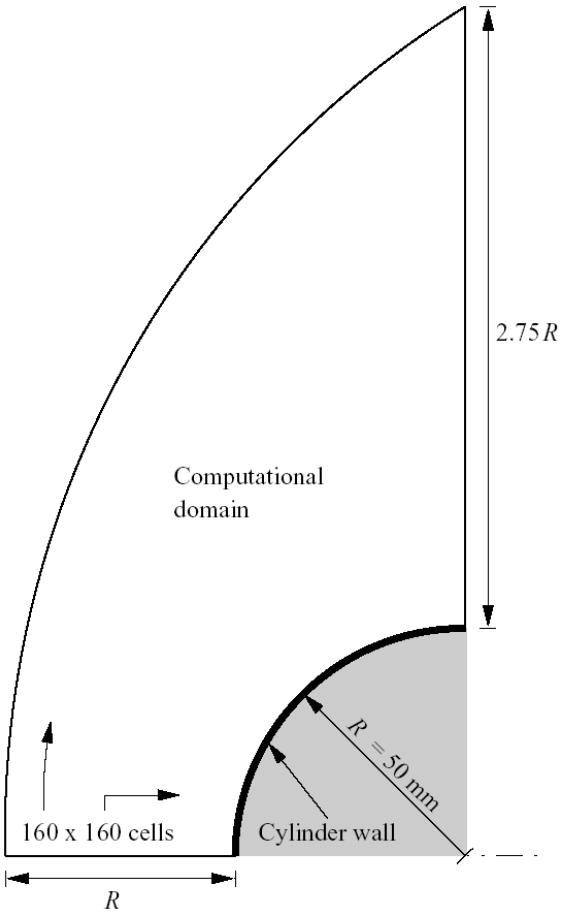

Fig. 2. Computational domain for the cylinder cross-flow problem. Our mesh comprises 160×160 cells

The flow is simulated in 2D as symmetric about a horizontal centreline, extending around a 90° section of cylinder to the vertical (there may also be differences in surface velocity slip in the trailing region of the cylinder if there is geometrical dependency in the boundary conditions used, but this is the subject of future work). The numerical flow domain, shown in Figure 2, extends a distance R from the cylinder surface along the centreline to a distance 2.75R from the cylinder surface along the vertical line. The mesh is 160 cells in both the radial and circumferential directions, with a linear grading in the radial direction in which the radial thickness of the outermost layer of cells is 10× the thickness of the innermost layer of cells.

Our solver is developed using the Open Source Field Operation and Manipulation (OpenFOAM) C++ software [7]. OpenFOAM uses finite volume (FV) numerics to solve systems of partial differential equations ascribed on any 3D unstructured mesh of polygonal cells. Fluid flow solvers are developed within a robust, implicit, pressure-velocity, iterative solution framework.

For compressible flow, the iterative solution framework is for density, momentum, total energy and pressure. The FV discretisation maintains a compact computational molecule for the orthogonal component of the Laplacian terms, which corresponds to Rhie and Chow interpolation in the pressure equation [8]. The dependent fields in convection terms are interpolated using the MUSCL TVD scheme [9]. The temporal derivative is discretised using a two-time-level Euler Implicit scheme.

We show results from two different simulations: the first using the conventional form of the velocity slip boundary condition (2), the second using the general form of the boundary condition (1). Both simulations were initially performed using the Smoluchowski temperature jump condition [10] with the accommodation coefficient and surface temperature specified above.

Slip boundary conditions on the cylinder wall are implemented within OpenFOAM's structure of generic boundary condition types. The Maxwell velocity slip condition is derived from a generic 'partial slip' type, i.e. a mixed fixed-value (Dirichlet)/slip (symmetry) condition. The Schmoluchowski temperature jump condition is derived from a generic implementation of a mixed (Robin) fixed value/fixed normal gradient condition.

We specified the boundary conditions on other regions as follows: all solution variables at the inlet boundary are fixed at the freestream conditions; at the outlet, a zero normal gradient is imposed on all solution variables; the centreline boundary is a symmetry plane condition.

The two simulations were run with a time-step of 15 ns, corresponding to a maximum flow Courant number of 0.1. The solutions reached steady-state in a problem time of 0.7 ms, equivalent to approximately 19 sweeps of the domain in the freestream region of the flow. Convergence was judged as achieved when the residuals had fallen by five orders of magnitude.

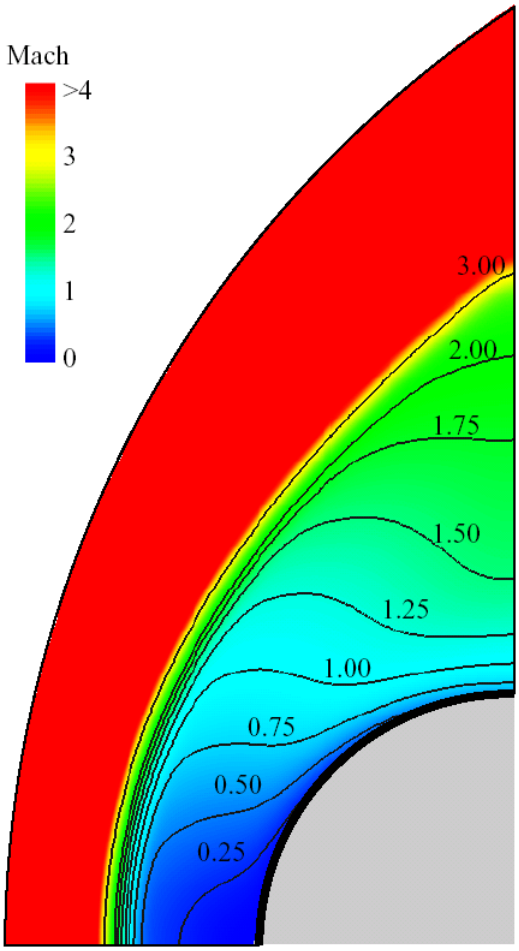

Fig. 3. Typical results from the OpenFOAM calculation around the leading edge of a cylinder; contours of Mach number labelled

A typical converged result is shown in Figure 3, which shows contours of Mach number around the leading edge of the cylinder (in this case using the general Maxwell slip condition). The bow shock is clearly evident.

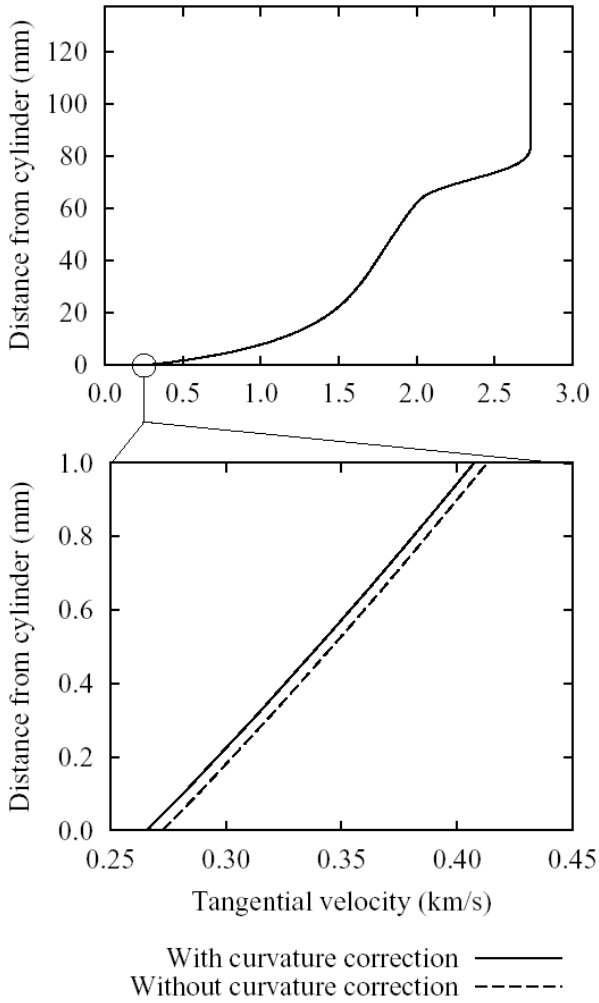

Fig. 4. Dimensional tangential velocity profiles in cylindrical cross flow. Comparison of results using conventional slip (- -) and Maxwell's general slip (—) boundary conditions

A more helpful figure for our purposes is Figure 4, which shows the predicted tangential velocity at the point on the cylinder at the far right boundary in Figure 2, varying with the normal distance away from the cylinder surface. The magnified section in Figure 4 shows the variation in tangential velocity close to the cylinder surface. Figure 5 shows how the velocity slip calculated at the wall varies along

the surface of the cylinder. This shows the consequences of the geometry-dependence of slip: there is up to a 2.1% difference in the calculation of slip at the wall between simulations using general Maxwell slip (1) and conventional slip (2). This accumulating error between the different velocity slip solutions is likely to have consequences in predictions of the trailing edge flow, or in the simulation of any aerodynamic surfaces beyond the right hand boundary of Figure 2.

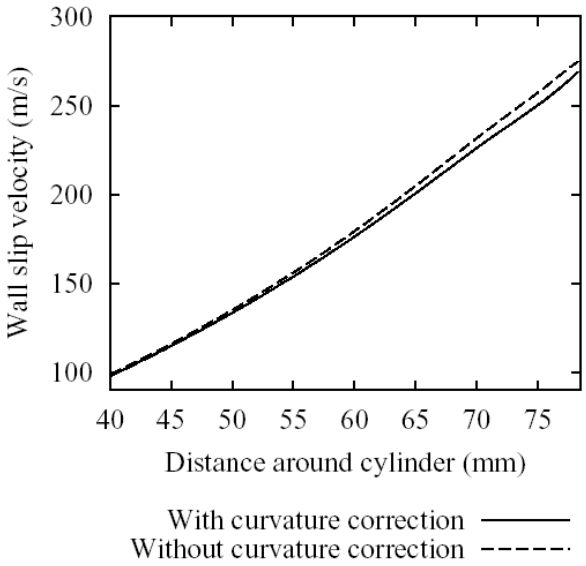

Fig. 5. Predictions of the velocity slip along the latter part of the circumference of the cylinder leading edge; conventional slip (- -) and Maxwell's general slip (—); *Smoluchowski temperature boundary conditions*

While this difference is fairly small in this test case, it is important to consider that the difference increases with the magnitude of the slip velocity. This is due to the fact that an increase in slip velocity leads to a decrease in normal gradient, thus increasing the relative contribution of the additional geometrical terms in the boundary condition. Increasing the boundary layer thickness by increasing the wall temperature has a similar effect.

Figure 6 shows results from the same test case, but this time using an adiabatic boundary condition at the cylinder surface. Here the difference in slip velocity along the cylinder surface is 7.5% at the far right boundary.

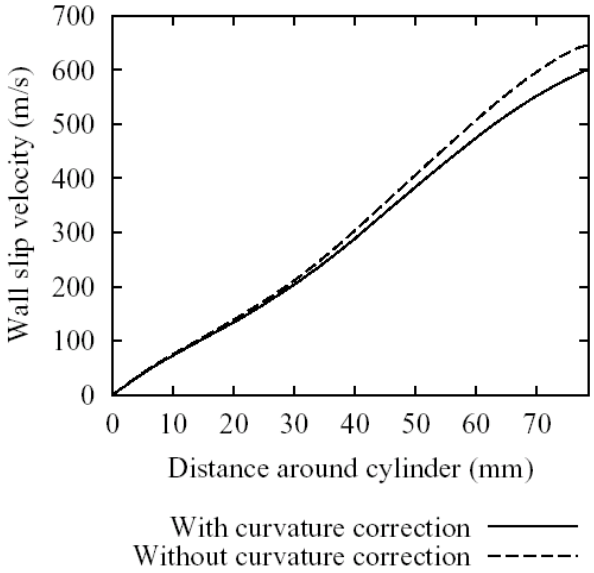

Fig. 6. Predictions of the velocity slip along the circumference of the cylinder leading edge; conventional slip (- -) and Maxwell's general slip (—); *adiabatic boundary conditions*

It should be noted that this geometry dependent slip has been calculated for the case of a simple cylinder only. Other surfaces where there is a streamwise variation in wall-normal velocity, either due to some streamwise curvature in the surface, or if the surface is moving normal to the flow (e.g. ailerons or rudders) will require simulations that incorporate the full Maxwell slip condition.

Conclusions

We have shown that numerical simulations of rarefied flows that use the conventional form of the velocity slip condition at bounding surfaces are likely to miss certain flow field information in complex geometries. We are extending this work to examine the benchmark 25°/55° biconic flow problem, where the point of intersection of the two cones leads to an additional geometry-dependent slip term which other simulations have ignored, but which may

have some consequences in modelling the flow field.

Finally, the Navier-Stokes-Fourier equations were used to derive equation (3), but these make very poor predictors of the viscous stress and heat flux close to a surface in a rarefied flow [1]. We hypothesise that better predictions of the slip velocity and temperature jump at the surface could be obtained by using higher-order approximations to the viscous stress and heat flux (e.g. the Burnett or Grad equations) appropriate for the highly non-equilibrium flow in the near-wall region [6].

Acknowledgements

The authors would like to thank: Steve Daley of the Defence Science and Technology Laboratory (Dstl), UK; Duncan Lockerby of Brunel University, UK; David Emerson and Robert Barber of Daresbury Laboratory, UK. This work is funded in the UK by the Engineering and Physical Sciences Research Council and Dstl under grant no. GR/T05028/01.

References

[1] Lockerby D.A., Reese J.M., Gallis M.A. Capturing the Knudsen layer in continuum-fluid models of non-equilibrium gas flows. *AIAA Journal*, 43(6), 1391-1393, 2005.

[2] Maxwell J.C. On stresses in rarified gases arising from inequalities of temperature, *Philosophical Transactions of the Royal Society of London*, 170, 231-256, 1879.

[3] Wang W.-L., Boyd I.D. Hybrid DSMC-CFD simulations of hypersonic flow over sharp and blunted bodies. *AIAA paper* 2003-3644, Orlando, Florida, 2003.

[4] Zuppard G, Paterna D. Influence of rarefaction on the computation of aerodynamic parameters in hypersonic flow. *Proc. Institution of Mechanical Engineers G (Journal of Aerospace Engineering)*, 216, 277-290, 2002.

[5] Agarwal R.K., Yun K.-Y., Balakrishnan R. Beyond Navier-Stokes: Burnett equations for flows in the continuum-transition regime. *Physics of Fluids*, 13(10), 3061-3085, 2001.

[6] Lockerby D.A., Reese J.M., Emerson D.R., Barber R.W. Velocity boundary condition at solid walls in rarefied gas calculations. *Physical Review E*, 70, art. No. 017303, 2004. http://www.openfoam.org.

[7] Rhie C.M., Chow W.L. A numerical study of the turbulent flow past an isolated airfoil with trailing edge separation. *AIAA paper* 82-0998, St. Louis, Missouri, 1982.

[8] Van Leer B. Towards the ultimate conservative difference scheme, V: a second-order sequel to Godunov's method. *Journal of Computational Physics*, 32, 101-136, 1979.

[9] Von Smoluchowski M. Über wärmeleitung in verdünnten gasen. *Annalen der Physik und Chemi*, 64, 101-130, 1898